Polymer 51 (2010) 5323–5331

Contents lists available at ScienceDirect

Polymer

journal homepage: www.elsevier.com/locate/polymer

Immobilization of polyisobutene in semi-interpenetrating polymer network architecture

Benjamin Davion, Cédric Vancaeyzeele, Odile Fichet*, Dominique Teyssié

Laboratoire de Physicochimie des Polymères et des Interfaces (LPPI), Université de Cergy-Pontoise, Institut des matériaux, 5 mail Gay-Lussac, Neuville-sur-Oise, 95000 Cergy-Pontoise Cedex, France

ARTICLE INFO

Article history:
Received 7 February 2010
Received in revised form
1 September 2010
Accepted 6 September 2010
Available online 21 September 2010

Keywords:
Polyisobutene
Semi-interpenetrating polymer networks
Flow inhibition

ABSTRACT

The entrapment of linear polyisobutene (PIB) in semi-IPN architecture is shown to be as efficient as it is in cross-linkable telechelic PIB based full IPN architectures as far as the suppression of cold flow is concerned. Indeed, homogeneous linear PIB/cross-linked polycyclohexylmethacrylate (PCHMA) semi-IPNs containing from 20 to 70 wt% PIB and synthesized without solvent show no cold flow and higher mechanical properties than those of linear PIB or 50 wt% PIB containing blend. In addition, the particular barrier properties toward gas and water are preserved. Those properties arise from the phase co-continuity morphology of the semi-IPN materials which moreover compares with that of corresponding IPNs. A systematic study of the synthesis conditions (nature of the initiator, temperature, cross-linking density) showed that the reacting mixture viscosity is an important parameter that controls the phase separation degree in the final material.

1. Introduction

Polyisobutene (PIB) is an important polymer both commercially and from a fundamental point of view regarding its peculiar physical properties. Indeed its thermal stability, resistance to weathering and UV light [1], and excellent gas barrier properties make it a choice elastomer in fields such as wrapping food and flooring road. As far as unusual physical properties is concerned low temperature relaxation [2,3] and the unusual dependence of PIB fragility with the molecular weight [4], these anomalous behaviours remain difficult to explain fundamentally. Nevertheless, polyisobutene materials exhibit poor mechanical properties due to creeping, low resistance to impact and penetration. Moreover PIB is not resistant to organic components such as solvents, lacquers, fats and oils. Thus, most applications require that polyisobutene preferably be immobilized inside a material.

In order to immobilize PIB, different strategies can so be used. For instance, the elaboration of PIB combinations with various polymers has been thoroughly investigated through diblock [5] and mostly triblock [6–9] copolymer synthesis leading to compatibilizing agents, thermoplastic elastomers (TPE), or biomaterials [10]. For example, Storey et al. synthesized a series of linear and three-arm star poly (styrene-*b*-isobutene-*b*-styrene) block copolymers with various block compositions via living carbocationic polymerization [11]. From these block copolymers, ionomer block copolymer have been obtained by polystyrene block sulfonation. After sulfonation, physical cross-linking remains stable at temperature higher than the Tg of polystyrene and tensile modulus and strength are increased [12–14].

Now of course the strategy of entrapping PIB in a material has also gone through the elaboration of networks. Indeed PIB based copolymers can be as well cross-linked leading to the co-network formation. Thus, Kennedy et al. have reported the synthesis of PIB/poly(dimethylsiloxane)(PDMS) co-networks [15–17]. In this material, PDMS chains are cross-linked through allyl-trifunctional polyisobutene via a hydrosilylation reaction. Bicomponent new nanostructured co-networks of poly(ethyl acrylate) [18], poly(2-hydroxyethylmethacrylate) [19] or poly(N,N-methylacrylamide) [20] cross-linked with α,ω-dimethacrylic PIB have been tested as drug delivery devices. Poly (ethyleneoxide)-linked-polyisobutene co-networks were also prepared from condensation of hydroxy-telechelic three-arm star PIB with isocyanate telechelic polyethyleneglycol [21].

PIB can be also immobilized into an interpenetrating polymer network (IPN) architecture which is defined as the combination of cross-linked polymers synthesized in juxtaposition [22,23]. Thus, PIB networks have been combined with polymethylmethacrylate [24], polystyrene [25] and poly(cyclohexyl methacrylate) [26] networks. The entrapment of cross-linked polyisobutene in IPN architecture is efficient and materials show interesting potential applications [27].

* Corresponding author. Tel.: +(33) 1 34 25 70 50; fax: +(33) 1 34 25 70 71.
E-mail address: odile.fichet@u-cergy.fr (O. Fichet).

0032-3861/$ – see front matter © 2010 Elsevier Ltd. All rights reserved.
doi:10.1016/j.polymer.2010.09.015

Be it linear or multiple arm copolymer synthesis or network or IPN design, either ionic polymerization mechanisms or ionic synthesis of telechelic PIB are prerequisite for realizing the desired immobilization strategy of PIB. Now a simpler route can be envisaged namely the elaboration of semi-Interpenetrating Polymer Network (semi-IPN) architectures in which PIB would be entrapped as a linear component in a partner network [23]. The advantage of semi-IPNs over IPNs in the case of PIB based architecture is that a no-functional linear PIB with middle/high molecular weight could be included into this architecture. The phase separation observed in the semi-IPN could be limited by a fast polymerization/cross-linking reaction of the partner network which would freeze the polymer chains before they can express their natural mobility. On the other hand, a drawback of semi-IPNs over IPNs is that, in IPN architecture, cold flow is totally prevented because of the cross-linked entangled state of both polymer partners. Due to the particular PIB flow property, a hazardous leaking out of the material of the linear polymer cannot be ruled out in the PIB based semi-IPNs. Another question arises as to whether the "interesting" properties of PIB will be preserved in the semi-IPN architecture. One of the possible solutions for meeting this challenge is to devise synthetic pathways leading to a maximized "clamping" of PIB within the partner polymer network promoting phase domains the size of which approach those of full IPNs preventing the natural PIB cold flow. On the other hand the design of semi-IPNs exhibiting phase co-continuity or near so would favour preserving PIB unique characteristics such as gas barrier properties.

Another challenge will be to avoid the use of solvent in an attempt to carry out environmental friendly synthesis which moreover could be carried out in *one pot* in some applications [28]. Thereby linear PIB must be soluble in the precursors of the partner polymer network. On the other hand, the aimed size of the phase domains must be as small as possible (<1 μm) in order to obtain a near to homogeneous material. This property can be reasonably expected if the interactions between linear PIB and polymer network are strong enough and would also contribute to lessen the possible PIB leakage phenomenon. In this respect poly(cyclohexylmethacrylate) (PCHMA) was chosen specifically because its solubility parameter value is very close to that of PIB (18.7 and 18.5 $MPa^{1/2}$ [29] respectively). In addition, CHMA monomer is a good solvent for PIB (PIB solubility higher than c.a. 4 gm L^{-1} in CHMA) hence the semi-IPN elaboration can be carried out without solvent.

The synthetic strategy for entrapping linear polyisobutene in PIB/PCHMA semi-IPN architecture is described here. The advantages and disadvantages of this type of architecture are compared with parent PIB based full IPNs from the flow properties, morphology and mechanical point of view. The first part of this study is devoted to the synthesis conditions of semi-IPNs. A detailed analysis is made of two particular synthesis parameters – nature of the radical initiator and polymerization time – which will help optimizing the properties of the resulting semi-IPNs. Then, the effects of cross-linking density of the methacrylic network on the semi-IPN properties are studied. The third part is devoted to the modelling of the semi-IPN morphology from the thermomechanical analysis data and the comparison with features evidenced by TEM. Finally, mechanical properties and morphologies of PIB based semi-IPNs and those of the corresponding IPNs previously made from telechelic PIB are compared.

2. Experimental part

2.1. Material

Oppanol B150G (Mn = 425,000 g mol^{-1} BASF data) described as high molar weight PIB showing no cold flow and Oppanol B15SFN (polyisobutene or PIB in the text) a middle molar weight PIB (Mn = 25,000 g mol^{-1}; polydispersity index (PDI) = 2.4 determined by SEC – polystyrene standard) showing important cold flow at room temperature were kindly provided by BASF. Cyclohexyl methacrylate (CHMA–Aldrich), ethylene glycol dimethacrylate (EGDMA–Aldrich) and dichloromethane (CH_2Cl_2, Carlos Erba) were used as received. Radical initiators benzoyl peroxide (BPO, Jansen) and dicyclohexylperoxydicarbonate (DCPD, Groupe Arnaud) were dried under vacuum before use.

2.2. Semi-IPN, blend and IPN synthesis

A PIB/PCHMA (50/50 wt/wt) semi-IPN was synthesized as follows: 2 g PIB, 2 g cyclohexylmethacrylate (CHMA) and 0.12 g EGDMA (5 mol% with respect to methacrylate monomer) were stirred slowly (50 rpm) in a reactor under argon atmosphere at 25 °C. Then, 2 mol% radical initiator with respect to methacrylate monomer was dissolved in the mixture which was then poured into a mould made from two glass plates clamped together and sealed with a 1 mm thick Teflon® gasket. The synthesis was carried out in an oven at temperatures according to radical initiator for different curing times. Semi-IPNs with different PIB contents ranging from 20 to 70 wt% were synthesized keeping the same proportions between monomer, cross-linker and initiator for PCHMA network. All investigated PIB/PCHMA compositions are reported in weight by weight ratio. Thus, a semi-IPN obtained from a mixture of 0.70 g PIB and 0.30 g CHMA will be noted PIB/PCHMA (70/30) semi-IPN.

PIB/PCHMA 50/50 blends were synthesized identically except that EGDMA was not included in the reacting mixture.

PIB/PCHMA IPNs synthesized for comparison were elaborated according to a procedure previously described [26] adapted to this study. Briefly, α,ω-dihydroxypolyisobutene (Mn_{SEC} = 4200 g mol^{-1}; PDI = 1.2 in THF with PS as external standard) and a pluri-isocyanate cross-linker (Desmodur N3300–Bayer) were mixed with CHMA and EGDMA (5 mol%) under argon. Then BPO (2 mol%) and a dibutyltindilaurate catalyst (1.3 mol% DBTDL with respect to PIB terminal OH groups) were added and the mixture was molded as the semi-IPNs. The curing program was 6 h at 60 °C, 25 min at 80 °C and 5 min at 100 °C.

2.3. Analytical techniques

Viscosity measurements were performed with a Brookfield Viscosimeter (DV-I Prime) at 40 and 80 °C. They were carried out on synthesis mixtures leading to PIB/PCHMA semi-IPN in which radical initiator was not added. However hydroquinone was added to prevent any polymerization in the medium.

Real time near infrared spectroscopy monitoring was performed on a Brüker spectrometer (Equinox 55) in the range 7000–4000 cm^{-1} by averaging 10 consecutive scans with a resolution of 4 cm^{-1}. The IR cell was inserted in an electrical heating jacket with an automatic temperature controller (Graseby Specac). The sample was cured in a specially designed and thermally controlled cell bracket (Eurolabo). The PCHMA network formation was followed by the disappearance of the H–C=C overtone absorption bands of the methacrylate group at 6163 cm^{-1} [30] integrated between 6255 and 6075 cm^{-1}. The peak area is directly proportional to the reagent concentration (the applicability of Beer Lambert law has been verified), thus the conversion-time profiles were easily derived from the spectra recorded as a function of time. The conversion of reactive bonds (p) can be calculated as

$$p = 1 - \frac{A_t}{A_o} \quad (1)$$

from the absorbance values (A) where the subscripts *0* and *t* denote reaction times.

The soluble fraction contained in the material (uncross-linked material) was extracted in a Soxhlet with CH_2Cl_2 for 48 h, PIB being soluble in this solvent. After extraction, the sample was dried under vacuum and then weighed. The extracted content (*EC*) is given as a weight percentage:

$$EC(\%) = \frac{(W_0 - W_E)}{W_0} \times 100 \quad (2)$$

The soluble fractions were analyzed by ^1H NMR. Thus the extent of covalent bond formation in the networks and semi-IPNs can be quantified.

Cross-linking density calculations: The M_c value for a given cross-linker amount is calculated as:

$$M_C = \frac{n_{CHMA} \times M_{CHMA}}{2 \times n_{EGDMA}} \quad (3)$$

where n_{CHMA} and n_{EGDMA} are the number of moles of CHMA and EGDMA introduced in the reaction mixture, respectively. The factor 2 corresponds the number of methacrylic groups of EGDMA. M_{CHMA} is the molar weight of CHMA.

The O_2 and water gas permeation of different materials were carried out in BASF according to the standards ASTM D 3985 and ASTM F-1249, respectively.

Dynamic Mechanical Thermal Analysis (DMTA) measurements were carried out with a Q800 model (TA Instruments) operating in tension mode. Experiments were performed at a frequency of 1 Hz and a heating rate of 3 °C min^{-1} from −100 to 200 °C. Typical dimensions of the samples were 30 mm × 5 mm × 1 mm. The set up provides the storage and loss moduli (E′ and E″) and the damping parameter or loss factor (tanδ) measured at 0.05% deformation in the linear domain.

The creep recovery measurements were carried out with the same DMTA apparatus. First, the temperature was equilibrated for 5 min at 30 °C and then a 0.05 MPa stress was applied to the sample for 10 min. The chosen stress is low in order to set the deformation in the linearity domain where the sample is reversibly solicited. Finally, the stress was stopped after 10 min and the sample length evolution was recorded during the next 20 min.

Transmission electron microscopy was carried out in BASF on cryomicrotomed samples and RuO_4 was used as contrast agent which selectively attaches on the PCHMA ester function.

3. Results and discussion

3.1. Semi-IPN synthesis

All the PIB/PCHMA semi-IPNs were synthesized from linear PIB (Mn = 25,000 g/mol-PDI = 2.4), CHMA monomer being used both as the precursor of the PIB partner network and as solvent in the *one pot* synthesis. The polymerization/cross-linking of CHMA with ethylene glycol dimethacrylate (EGDMA) proceeds through free-radical mechanism leading to the formation of the corresponding polymethacrylate network within PIB.

First the efficiency of two initiators was assessed by comparing the yields of completion of the polymerization and cross-linking in the presence of 2 mol% BPO or DCPD as free-radical initiators. The synthesis temperature was set at 80 and 40 °C for BPO and DCPD respectively. Under those conditions, radical flux should be similar in both systems based on the same dissociation constant value ($k_d = 10^{-5}$ s^{-1} and $t_{1/2} = 10$ h for DCPD and BPO [31]). Of course the reactive medium viscosities are different at those two temperatures as measured for different initiator free PIB/CHMA mixtures at 40 and 80 °C (Table 1). For instance, the viscosity of a PIB/CHMA (50/50) mixture is equal to 66.8 and 17.8 Pa.s at 40 and 80 °C respectively.

Table 1
Viscosity of different initiator free PIB/CHMA mixtures and methacrylate conversion rate measured on the corresponding semi-IPNs at different temperatures.

PIB/CHMA proportion		0/100	30/70	50/50	70/30
Viscosity (Pa s)	40 °C	<1	3.4	66.8	1231.5
CHMA conversion rate (mol min^{-1})		0.433	0.180	0.089	0.028
Viscosity (Pa s)	80 °C	<1	1.1	17.8	201.0
CHMA conversion rate (mol min^{-1})		3.178	1.833	0.941	0.389

The effect of the viscosity value of the medium on the PCHMA network formation leading to semi-IPNs was studied by real time near IR disappearance of the H—C = C overtone absorption bands at 6163 cm^{-1} monitoring at 40 and 80 °C for DCPD and BPO initiators respectively [26,30]. The methacrylate function conversions were recorded versus time (Fig. 1).

When DCPD is chosen as free-radical initiator, the conversion curves have the same shape whatever the semi-IPN composition (Fig. 1A). An inhibition period probably due to the oxygen traces in the reaction mixture is observed the duration of which increases with decreasing starting PCHMA amount, hence with increasing viscosity (argon degassing does not prove efficient enough in order to get rid of residual oxygen due to high viscosity). After the inhibition delay, the conversion rates are equal to 0.180, 0.089 and 0.028 mol min^{-1} for PIB/PCHMA (30/70), (50/50) and (70/30) semi-IPNs, respectively i.e. proportional to CHMA weight fraction under

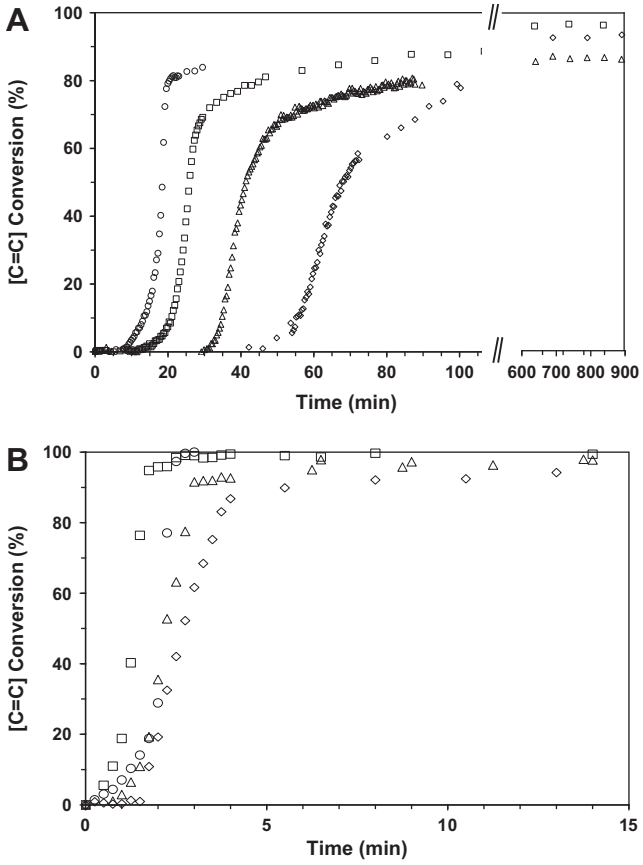

Fig. 1. Conversion of the methacrylic function in a mixture of precursors of PIB/PCHMA (0/100) (○), (30/70) (□), (50/50) (△) and (70/30) (□) semi-IPNs initiated with 2 mol% (A) DCPD at 40 °C and (B) BPO at 80 °C versus time measured by real time monitoring near IR spectroscopy.

those synthesis conditions. These rate values are lower than that of the PCHMA single network as expected (without PIB-0.433 mol min^{-1}). Conversion values reach a pseudo plateau at about 80% whatever the PCHMA proportion after 20 min to 2 h according to the PIB/PCHMA composition. However, the methacrylate conversion continues to increase very slowly up to 85–95% after 600 min at 40 °C.

When BPO is used as free-radical initiator, the conversion-time curves at 80 °C show the same outline than with DCPD initiator (Fig. 1B). However, the inhibition periods are considerably lower (less than 2 min). Thus the prominent parameter in the inhibition delay rather seems to lie in the decrease of the initiator efficiency due to the viscosity of the medium. Potential cage reaction of the initiator-derived radicals, i.e. primary radical termination and transfer to initiator relative importance, depends on monomer concentration and medium viscosity [32]. Thus, the difference in viscosity at 80 °C (temperature when BPO is used) and 40 °C (when DCPD is chosen) seem sufficient to account for the observed phenomenon.

3.2. Influence of initiators

After the inhibition period, the methacrylate conversion rate is again proportional to CHMA proportion in the semi-IPN when BPO is used as the initiator (Table 1). However, for an identical CHMA concentration, the conversion rate is faster with BPO initiator than with DCPD although a similar radical flux is generated in the reactive medium under the chosen experimental conditions (Table 1). Finally the plateau conversion is higher with BPO initiator (between 90 and 100%) than with DCPD (80%). This behaviour can be also accounted for by the modulation of the initiator efficiency according to the medium viscosity, and early loss of free-radicals due to oxygen absorption, as noted above.

The influence of the initiator nature on the thermomechanical properties (in particular tanδ-temperature curves) of semi-IPNs with various compositions has been then examined after a 16 h synthesis at 40 °C and 80 °C with DCPD and BPO as radical initiators. Firstly, the half-height width (ΔT) of the PCHMA single network relaxation centered at +140 °C is larger when PCHMA network is initiated with DCPD (ΔT = 37 °C) instead of BPO (ΔT = 26 °C-Table 2). This behaviour is found again in the semi-IPNs. For example, the half-height width of PIB/PCHMA (50/50) semi-IPN is equal to ΔT = 34 °C and ΔT = 48 °C when PCHMA network formation is initiated with BPO and DCPD, respectively (Table 2).

Conversely the bimodal shape of the PIB rich phase tanδ relaxation (−30 °C relaxation associated to the PIB cooperative backbone motion and a low temperature shoulder (−50 °C) associated to the PIB end local chain motion [33–35]) is significantly affected by the initiator nature. This relaxation remains quite broad as in other PIB based materials [6,12]. However when DCPD is used as initiator, the tanδ peak intensity is equal (for lower PIB proportions) to lower than that observed when BPO initiates the PCHMA network formation. The difference is more important the more the PIB proportion increases. This shows that the PIB cooperative backbone motion is less hindered when PCHMA polymerization is initiated with BPO and suggests a more important phase separation between PIB and PCHMA network. The BPO mediated synthesis at 80 °C yields a viscosity about four times lower than that at 40 °C. This DMTA analysis shows that for PCHMA based PIB semi-IPNs the nature of the initiator and/or the reaction temperature will play a role in addition to the gross quantity of radicals.

Table 2
tanδ peak half-height width (ΔT) of the PCHMA network and linear PIB relaxation in the semi-IPNs and the PCHMA single network.

PIB/PCHMA semi-IPN composition		70/30	50/50	30/70	0/100
PCHMA tanδ peak half-height width ΔT (°C)	DCPD initiated	58	48	44	37
	POB initiated	52	34	36	26
PIB tanδ peak half-height width ΔT (°C)	DCPD initiated	41	35	24	–
	POB initiated	46	36	24	–

3.3. Soluble fractions

The soluble fractions contained in the resulting semi-IPNs were measured as to witness the degree of completion of the PCHMA polymerization/cross-linking reaction and the strength of PIB entrapment in the semi-IPNs after 16 h reaction at 80 °C. In each case the initially introduced amount of PIB is expected to be totally recovered by solvent extraction. When BPO is used as the initiator the plot of the amount of soluble material shows slight deviation from a straight line with slope equal to 1 (Fig. 2). When PIB contents exceed 60 wt% free PCHMA oligomers are detected in the extracted products by ^{1}H NMR suggesting that a 5% amount EGDMA cross-linker or the polymerization temperature (80 °C-16 h) might be not sufficient in order to complete the PCHMA network in highly viscous media (Fig. 2(□)). When PIB content is ≤50 wt% the exact amount of introduced linear PIB is recovered (as checked by ^{1}H NMR) witnessing the completion of the CHMA polymerization reaction and the absence of PIB/PCHMA cross-reaction.

In the case where DCPD is used as the initiator the soluble material amount disagrees with the expected one in a reproducible way being consistently lower than expected especially when PIB amount is lower than 50 wt% which could illustrate that a significant PIB proportion (5–12 wt% according to the PCHMA proportion) is either very tightly entrapped in the material or covalently linked to the PCHMA network (Fig. 2 (○)). This hypothesis is supported by recent observations [36] on the elaboration of polymers from H-labile bearing monomer initiated with DCPD where an over expressed cross-linking reaction is involved. Moreover a PIB/PCHMA (50/50) blend where DCPD or BPO are used alternatively as initiators for the polymerization of CHMA (without EGDMA cross-linker) lead to totally different materials: the blend initiated with BPO is totally soluble as expected for two linear polymers whereas the blend initiated with DCPD leads to only 38 wt% PIB soluble fraction (instead of 50 wt%) supporting the hypothesis of a cross-linking reaction between the two partner polymers. Thus DCPD was definitely discarded as an initiator in the preparation of PIB/PCHMA semi-IPNs and BPO was selected instead.

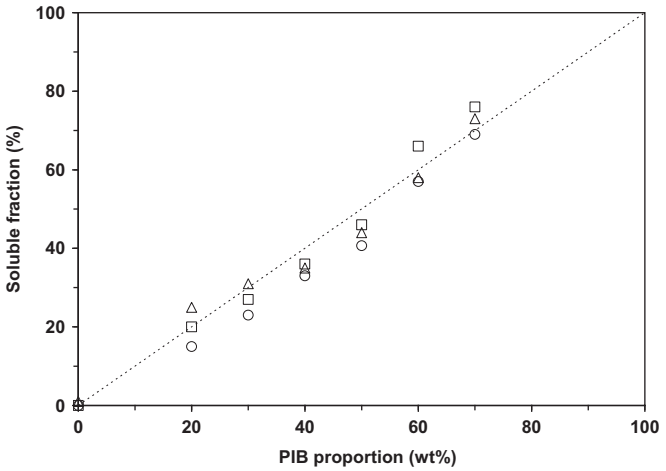

Fig. 2. Extractible amounts as a function of PIB weight proportion in PIB/PCHMA semi-IPNs initiated with 2 mol% DCPD (○) 40 °C-16 h, BPO (□) 80 °C-16 h and BPO (△) 80 °C-25 min + 100 °C-5 min.

The curing time of the BPO initiated semi-IPNs has been then optimized considering the excess amount of soluble material at high PIB (≥60 wt%) content and also the FTIR data (Fig. 1) show that over 90 wt% only of the methacrylate group double bonds in the reaction mixture convert within 10 min at 80 °C. A 5 min post-cure at 100 °C was selected for the synthesis of all the subsequent PIB/PCHMA semi-IPNs since it allows to get rid of a post polymerization appearing on DSC signal between 110 and 170 °C after an isothermal polymerization at 80 °C (Fig. 2(△)).

3.4. PIB entrapment

Due to the particular properties of PIB no prediction can be made about how strong the entrapping in the semi-IPN architecture which was chosen so as to entrap PIB inside a material and further compared with a full PIB/PCHMA IPN architecture reported earlier [26]. PIB efficient entrapping inside PCHMA network requires that the molecular weight between PCHMA cross-links (M_c) must be smaller than molecular weight between PIB entanglements (M_e) in order for each linear chain to be clamped several times between each entanglement. Molecular weight between entanglements (M_e) is of the order of 8000–9000 g mol^{-1} in linear PIB [37] which corresponds to a packing length of about 2 nm [38]. Thus, it would be preferable to entrap PIB into a PCHMA network with M_c from 500 to 2000 g mol^{-1} for the PIB chains to be clamped at least three times between each entanglement. From the Equation (3) reported in Experimental section, 5 mol% EGDMA cross-linker in CHMA leads to the formation of a network in which calculated M_c is 1680 g mol^{-1}.

Indeed a PIB/PCHMA (50/50) semi-IPNs synthesized with 1 mol % EGDMA leads to 55 wt% soluble fraction containing residual methacrylic oligomer chains (confirmed by ^{1}H NMR), showing that this amount of cross-linker is not sufficient to complete the network. For 5 mol% EGDMA (where M_c is 1680 g mol^{-1} i.e. the minimum value for sufficiently entrapping PIB) 48 to 52 wt% soluble fractions (Fig. 2(△)) are composed of linear PIB as confirmed by ^{1}H NMR analyses. Thus, as expected, the lowest the PCHMA M_c, the better PIB chains seem to be entrapped in PCHMA network.

The DMTA analysis performed on PIB/PCHMA (50/50) semi-IPNs cross-linked with 1, 2, 4, and 5 mol% EGDMA were then compared with similar measurements performed on a PIB/PCHMA blend where the entrapment of PIB is expected to be minimal (Fig. 3).

As expected, the semi-IPN in which PCHMA is cross-linked with 5 mol% EGDMA shows the highest storage modulus. In addition, whatever the cross-linking density, the semi-IPNs do not flow up to 200 °C. The tanδ value at the maximum of the PCHMA rich phase mechanical relaxation decreases from 2.3 to 1.6 when the EGDMA proportion with respect to CHMA increases from 0 to 5 mol%. Simultaneously, the Tα value of the PCHMA rich phase slightly increases from about 134 °C up to 142 °C which is characteristic of networks with increasing cross-linking densities [39]. The PIB cooperative backbone motions (Tα = −30 °C) are more important in the blend than in the semi-IPNs of identical composition. The tanδ is down shifted from 0.7 to 0.5 witnessing that a decrease in chain mobility depends upon the PCHMA cross-linked environment. Moreover the PIB tanδ peak is nearly not affected in shape neither intensity confirming that no cross-reaction occurs between PIB, EGDMA nor PCHMA under the studied conditions. All the following semi-IPNs have been synthesized with 5 mol% EGDMA.

3.5. Oxygen and water gas barrier properties

It seemed significant at this point to check whether the particular permeability property of PIB is kept in the semi-IPNs. The oxygen and water gas barrier properties were analyzed on linear PIB, PCHMA single network and PIB/PCHMA (50/50) semi-IPN. The O_2 permeation of PCHMA and PIB are 51400 and 84000 cm^3.μm m^{-2}.d^{-1}.bar^{-1} respectively. The semi-IPN permeation i.e. 56200 cm^3.μm m^{-2}.d^{-1}.bar^{-1} value lies close to the lower one i.e. that of PCHMA. Otherwise the water vapour barrier properties of PCHMA and PIB are equal to 571 and 45 cm^3.μm m^{-2}.d^{-1} respectively. The semi-IPN value is in between the former ones and equals 240 cm^3.μm m^{-2}.d^{-1}. The semi-IPN barrier properties result from both component polymers and PIB and PCHMA have very different barrier properties. The resulting semi-IPN takes advantage of the PIB water barrier properties and exhibits a behaviour close to that of the hydrophobic polymer. The PCHMA network included in the semi-IPN seems to behave similarly to the lone polymer (restricted chain mobility) and the resulting semi-IPN has a low O_2 permeation. So the (50/50) semi-IPN takes advantage of both polymer properties. Curiously the gas permeation properties that one hoped to keep in synthesizing a PIB based semi-IPN are even improved in this architecture. Examination of other semi-IPN compositions is in progress.

Finally, under these optimized experimental conditions relative weight proportions between PIB and the PCHMA network in final materials were varied from 20 to 70 wt% PIB. These samples have been characterized by their optical and thermomechanical properties and transmission electron microscopy.

3.6. Semi-IPN transparency

Same as the corresponding IPNs, all the PIB/PCHMA semi-IPNs are transparent whatever the partner weight proportions. Transmittance of all 1 mm thick semi-IPNs is about 87% between 400 and 800 nm and remains constant from 20 °C to 100 °C. The reflection and the diffuse transmission are equal to about 9% and 5%, respectively. However no conclusion with regard to the morphology can be drawn from this observation since the transparency originates in the

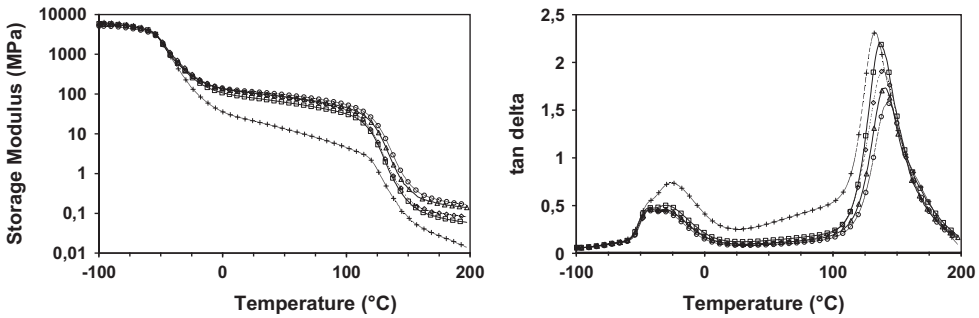

Fig. 3. Storage modulus (left) and tanδ-temperature curves recorded on PIB/PCHMA (50/50) semi-IPNs cross-linked with 1 mol% (□), 2 mol% (◇), 4 mol% (△) and 5 mol% (○) EGDMA. PIB/PCHMA (50/50) blend (+) is reported for comparison. Initiator: BPO 2 mol%.

fact that the two components have matching refractive indices i.e. 1.507 and 1.497 for PCHMA and PIB [40].

3.7. Creep recovery response

Cold flow properties were then studied at 30 °C by creep recovery experiments performed on PIB/PCHMA semi-IPNs, single PCHMA network and linear PIB (Oppanol B150G-Mn = 55000 g mol^{-1}) described as high molar weight PIB and usually taken as a reference for a PIB material showing no cold flow (Fig. 4).

The PCHMA single network is in a glassy state and does not deform. The value measured on linear high molecular weight PIB is equal to 6% strain and shows 90% recovery. The maximum strain values recorded on the semi-IPNs are very low (between 0.01 and 0.15% for 30 to 70 wt% PIB) compared with linear PIB and the process is reversible for all samples (between 100 and 94% recovery for 30 to 70 wt% PIB). These experiments confirm that the PIB/PCHMA semi-IPNs containing a PIB weight proportion lower than 70 wt% do not cold flow. Thus, even though PIB included in the studied semi-IPNs is middle molar weight it does not flow under the standard conditions contrary to that included in the PIB/PCHMA (50/50) blend.

3.8. Thermomechanical properties

The thermomechanical properties of PIB based semi-IPNs are reported in Fig. 5. The storage modulus (E′) – temperature curves confirm that the semi-IPNs do not flow up to 160 °C except for the PIB/PCHMA 70/30 composition. The storage modulus of linear PIB (Mn = 25000 g mol^{-1}) has been also reported for comparison. Due to the cold flow of this polymer, regular DMTA measurements as a function of temperature cannot be carried out. Thus the storage modulus values have been calculated at each temperature starting from shear modulus and elastic modulus reported in the literature [41] which are converted in storage modulus using Poisson coefficient equal to 0.5.

When the temperature is raised above −50 °C where the samples are considered to be in a rigid glassy state, the value of E′ decreases from about 3000 MPa to a plateau extending from 0 to 100 °C–120 °C. The plateau storage modulus values decrease from 1500 to 5 MPa when the PIB content increases from 20 to 70 wt%. The regular evolution of plateau height as a function of the PIB content is an indication of polymer phase co-continuity on the whole material. When the temperature is higher than 100 °C, the semi-IPN storage moduli decrease below 1 MPa at the polymethacrylate network mechanical relaxation temperature

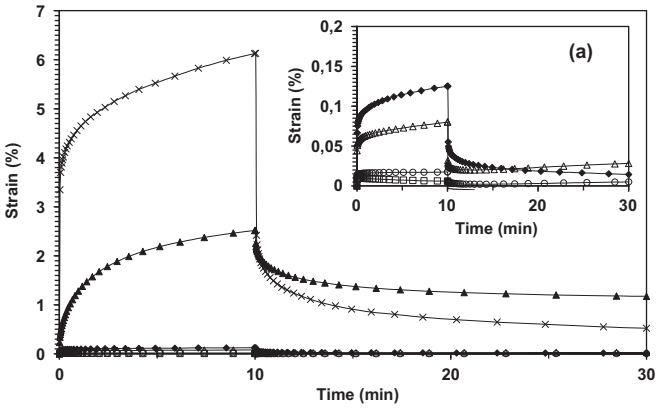

Fig. 4. Creep recovery experiments performed on PCHMA single network (○), PIB/PCHMA (□) (30/70), (△) (50/50), and (◆) (70/30) semi-IPNs. PIB/PCHMA (50/50) blend (▲) and linear PIB (Oppanol B150G-×) are reported for comparison. Stress: 0.05 MPa for 10 min at 30 °C. Insert (a): zoom between 0 and 0.2% strain.

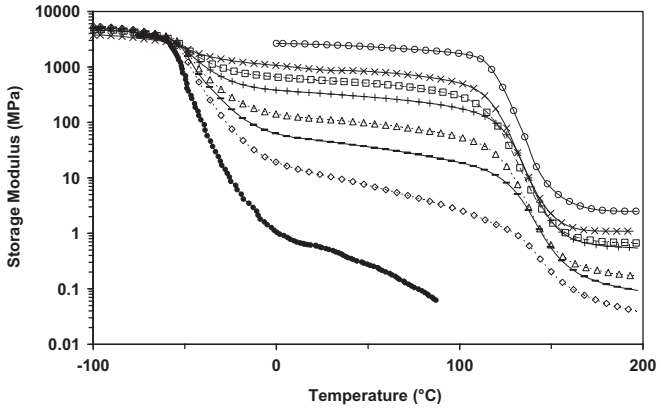

Fig. 5. Storage modulus - temperature curves recorded on (○) PCHMA single network, PIB/PCHMA (×) (20/80), (□) (30/70), (+) (40/60), (△) (50/50), (—) (60/40) and (◇) (70/30) semi-IPNs, (●) linear PIB (25,000 g mol^{-1}).

(Tα = +140 °C) and the semi-IPNs are in a rubbery state. The position of the rubbery plateau decreases from 1 to 0.03 MPa when the PIB proportion increases from 20 to 70 wt%. The (70/30) semi-IPN shows a different behaviour compared with that of the other semi-IPNs. For all the measurements, the strain applied to the sample is set at 0.05%. However, the apparatus does not succeed in keeping this strain which increases to 0.3% at 200 °C although the same stress is applied on the (70/30) semi-IPN. Thus the high PIB weight proportion semi-IPN starts flowing at temperature higher than 160 °C. Thus, the semi-IPN architecture leads to PIB based materials which do not show flow when the PIB proportion is lower than 70 wt% only. The semi-IPN storage moduli are higher than that of linear PIB whatever the semi-IPN composition above −50 °C.

The corresponding tanδ-temperature curves of PIB/PCHMA semi-IPNs in which the PIB proportion increases from 20 to 70 wt% are reported in Fig. 6. The tanδ values of linear PIB (Mn = 25,000 g mol^{-1}) calculated with the same procedure as the corresponding storage modulus have been also reported for comparison.

All semi-IPNs show two mechanical relaxations characterized by a tanδ peak located at the PIB and PCHMA network Tα temperatures. The mechanical relaxations are detected at about −30 and +140 °C and they are characteristic of linear PIB and PCHMA network rich phases, respectively. The PIB tanδ peak intensities in the semi-IPNs are much lower than that of pure PIB, and decrease with decreasing PIB proportion in the semi-IPN. This signal results from the superposition of a peak corresponding to local movements (Tα = −50 °C) and a second one characteristic of the PIB segmental motions (Tα = −30 °C) [33–35]. This PIB mechanical relaxation is strongly affected when PCHMA content increases to 80 wt% where only local movements (Tα = −50 °C) are still detected. Thus, the areas of −30 and −50 °C peaks have been calculated with a deconvolution software (Origin®) [42]. The area proportions of the peaks characteristic of PIB segmental motions are equal to 60, 66, 74, 90, 92, 95% of the total PIB peak in PIB/PCHMA (20/80), (30/70), (40/60), (50/50), (60/40) and (70/30) semi-IPNs, respectively, while the PIB mechanical relaxation corresponds to 98% segmental motions in pure PIB. While the segmental motion is predominant in pure PIB, it becomes strongly hindered when the PCHMA weight proportion increases. These results witness a strong interaction between PIB and PCHMA phases. From these calculations, it can be considered that about 38% of the present PIB is hindered by the PCHMA presence in the PIB/PCHMA (20/80) semi-IPN, for example. Thus the linear PIB/PCHMA network association cannot be considered as immiscible neither without polymer interaction (indeed two distinct phases are detected by DMTA analysis).

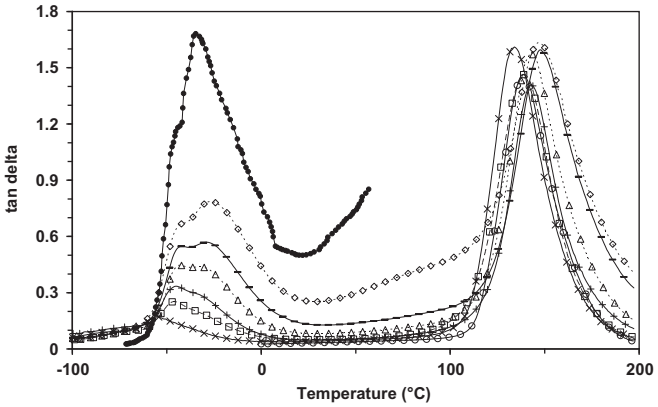

Fig. 6. tanδ-temperature curves recorded on (○) PCHMA single network, PIB/PCHMA (×) (20/80), (□) (30/70), (+) (40/60), (△) (50/50), (−) (60/40) and (◇) (70/30) semi-IPNs, (●) linear PIB (25,000 g mol^{-1}).

At higher temperatures, all semi-IPNs show a PCHMA network rich phase mechanical relaxation characterized by a tanδ peak centered at 140 °C. Unexpectedly, the peak intensity seems hardly affected by the PCHMA proportion in the semi-IPN although it is slightly shifted in temperature. In order to try and interpret this phenomenon, the molecular weight between PCHMA cross-links (M_c) in the semi-IPNs has been measured by swelling of the extracted semi-IPNs (i.e. totally freed from PIB) in $CHCl_3$ by using the Flory–Rehner equation [43]. It appears that the molecular weight between PCHMA cross-links (M_c) increases from 1730 g mol^{-1} in the single PCHMA network (which is close to the calculated $M_c = 1680$ g mol^{-1}) to 5950 g mol^{-1} in the PIB/PCHMA (60/40) semi-IPN while the same cross-linker molar content with respect to CHMA monomer is used for the synthesis. A similar behaviour has been observed by Sperling in polybutylmethacrylate/polystyrene semi-IPNs [44]. Thus, the higher the PIB weight proportion, the less the PCHMA cross-linking density is. This result can partially explain the irregular behaviour of the PCHMA main peak intensity in semi-IPN. Indeed, on the one hand, the PCHMA peak area decreases with decreasing PCHMA weight proportion. On the other hand, the PCHMA peak intensity and area would increase when the cross-linking density decreases and the network become less homogeneous, i.e. when PIB proportion increases. Both effects act in opposite way and this might explain the quasi constant intensity value of the PCHMA peak. Moreover the two phases in the material keep their typical mechanical relaxation temperature and thus do coexist separately. Indeed no interpenetrating phase between the two polymers appears in the semi-IPN which would be characterized by an intermediate mechanical transition in a temperature range between −30 °C (PIB) and +140 °C (PCHMA) as it was observed for PIB/PCHMA full IPNs [26].

Finally unusual is the behaviour of 70 wt% PIB material where the damping properties of the semi-IPN are distinctly affected by the PIB content between 20 and 100 °C with tanδ values reaching 0.3 to 0.5. But it was shown that this particular sample exhibits flown affirming that no cross-reaction occurs between PIB, EGDMA nor PCHMA below 160 °C. And thus PIB is not correctly entrapped in this case.

The manner the domains rich in one of the two polymers arrange i.e. the semi-IPN morphology, governs the mechanical properties of the material. The possible morphologies are a phase rich in one polymer dispersed in the other or two co-continuous phases, each morphology engendering particular mechanical features. Thus, from the DMTA measurements, morphology can be inferred by using mechanical models assuming a particular morphology, which will be confirmed subsequently by microscopy imaging.

Although some models have been established for polymer blends, numerous authors have found that they apply successfully to the description of IPN viscoelastic properties [45–47]. Four models have been considered in this work. These models allow calculating the shear modulus G_{MODEL} of a hard and a soft polymer mixture arranged in a given morphology from the G_{HARD}/G_{SOFT} ratio. These models assume no adhesion default between the phases and samples being macroscopically isotropic. According to Kerner model [48] spherical inclusions are dispersed over the whole composition range in a polymer matrix supposedly without interactions between the dispersed domains and the matrix. Budiansky model predicts a phase inversion at middle-range compositions [49]. The material morphology is supposed to be a continuous hard phase in which the soft phase is dispersed when its volume fraction is lower than 0.5 followed by a phase inversion when this volume fraction is higher than 0.5. The Coran-Patel model includes a fitting parameter, n, that can be related to phase inversion the position of which can differ from 0.5. For systems of variable morphology, $1-[(n-1)/n]$ probably indicates the approximate centre of a range of the volume fractions, wherein a phase inversion takes place [50,51]. Finally, Davies model [52] considers that both phases are co-continuous over the whole material.

First, the storage modulus values were extracted from the DMTA curves at 25 °C where PIB is taken as the soft polymer and PCHMA the hard one. Based on the E′ (Fig. 5) and the tanδ (Fig. 6) values at 25 °C, the tensile modulus E ($E = \frac{E'}{\cos\delta}$) and the shear modulus G ($G = \frac{E}{2(1+\nu)}$ where ν is Poisson coefficient) are successively calculated. Using shear moduli of 0.017 MPa for PIB [41] and 1240 MPa for PCHMA phases, the shear moduli of materials with hypothetical morphologies can be calculated from the different models (Fig. 7). Two shear moduli curves have been calculated from the Kerner model in one of which the hard PCHMA phase would be the matrix ($G > 30$ MPa over the whole composition range) or else the PIB would be ($G < 0.3$ MPa). The Budiansky model leads to low shear moduli (<0.1 MPa) at low PCHMA content and to higher moduli (>100 MPa) when this content increases over 50 vol%. The Coran-Patel model with the fitting parameter $n = 4.7$ leads to the same extreme values of shear modulus but with less abrupt phase inversion centered around $1-[(n-1)/n] = 21$ vol% PCHMA. By considering phase co-continuity and using the Davies model, G increases regularly from 0.2 to 300 MPa with the PCHMA content from 10 to 90 vol%. For extreme compositions, all models give converging shear moduli values and would not be

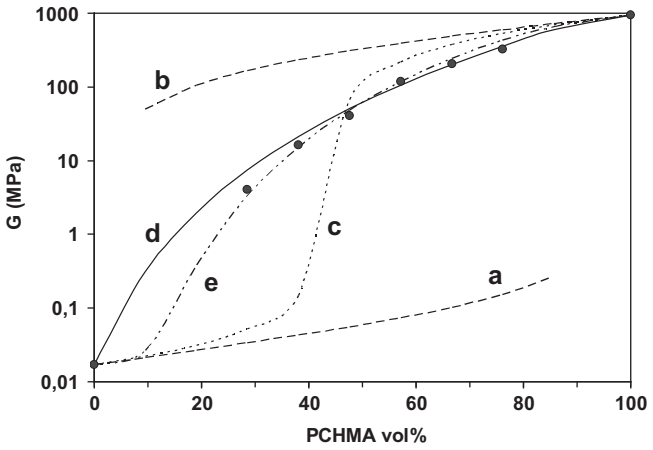

Fig. 7. Shear modulus versus PCHMA volume proportion in the PIB/PCHMA semi-IPNs. Kerner model in which (a) PIB is matrix and (b) PCHMA matrix, (c) Budiansky model, (d) Davies model, (e) Coran-Patel model ($n = 4.7$) and (●) shear modulus of PIB/PCHMA semi-IPN calculated from DMTA data.

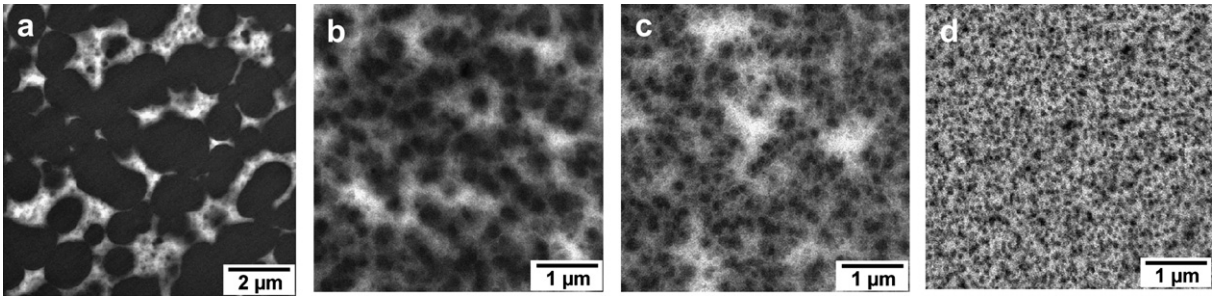

Fig. 8. TEM morphology images of PIB/PCHMA (a)(20/80), (b)(50/50), (c)(60/40) and (d)(70/30) 50 nm thick semi-IPNs. The PCHMA rich domains are stained with RuO_4 (in dark in the pictures). The scale of the left picture is twice larger than that of the others.

proportions were clear cut conclusions could be drawn when compared with experimental data.

Comparing experimental values extracted from the DMTA data on the PIB/PCHMA semi-IPNs (Figs. 5 and 6) and the model calculated values the Davies and the Coran-Patel models estimate very close values for PCHMA ratio higher than 50 vol%. Whereas data for semi-IPN with low PCHMA proportion follow the same tendency as those of the Coran-Patel model ($n = 4.7$) which stands for phase inversion around 21 vol% PCHMA. Unambiguously for intermediate PIB weight proportions (30–60 vol%) the mechanical features of the semi-IPNs are thus in good agreement with the PCHMA phase connectivity, i.e. progressively increasing stiffness with the PCHMA proportion without any material flow.

3.9. Transmission electronic microscopy

The PCHMA phase connectivity over a large composition range hypothesis has been strengthened by transmission electronic microscopy imaging of the morphology of four PIB/PCHMA (20/80), (50/50), (60/40) and (70/30) semi-IPNs (Fig. 8). The methacrylic partner was stained by RuO_4, thus the rich PCHMA phase appears dark and the clear domains on the picture are the PIB rich phase.

From these images, the PIB rich phase appears to remain continuous in the studied composition range.

In the PIB/PCHMA (20/80) semi-IPN (Fig. 8a) large (2 µm) PCHMA percolating spherical-like domains are dispersed in a continuous PIB phase. PIB and PCHMA phases are thus co-continuous at the 2 µm scale. If one re-examines the PIB rich phase in this particular composition dispersion of a number of smaller PCHMA domains the size of which is lower than 0.1 µm appears. This smaller domain morphology is detected whatever the semi-IPN composition as shown below for the other compositions.

For PCHMA proportions ranging from 50 to 30 wt% (Fig. 8b to d) the PCHMA phase domain size vary from about 0.3 µm to lower than 0.1 µm. The shape of the domains does not vary compared with the sample with the highest PCHMA proportion and the domains remain connected as well. Phase domain dimensions in this order of magnitude are smaller in size than those generally observed for copolymers or blends [53,54], but also for semi-IPNs [55].

Thus, although the size of the PCHMA phase domains is clearly a function of the composition, the morphologies detected by TEM microscopy on the different semi-IPNs seem to indicate that a PCHMA phase in the form of percolating connected domains dispersed in a continuous PIB phase is obtained whatever the semi-IPN composition.

Thus, the electron microscopy images suggest PIB and PCHMA co-continuity in agreement with the morphology of the semi-IPNs derived from the model study for proportion higher than 30 wt% PCHMA. Based on these TEM images, no conclusion is drawn about a potential phase separation mechanism by growth-nucleation or spinodal decomposition. Indeed, samples are thin slices and the observed shapes can mislead about the real shape (sphere, cylinder or short rod) of the phase domains in bulk [56].

In addition a pixel image analysis of black, white and different grey shades (GIMP 2.2® software) has been performed on the four micrographs leading to finer conclusions. In extreme compositions (Fig. 8a and d) it appears that the percentage the pure polymer component (PIB and PCHMA respectively) is far lower than the introduced one which means that the majority of the sample is composed of a combined PIB/PCHMA phase corroborating a phase co-continuity. In the two intermediate compositions i.e. PIB/PCHMA (50/50) and (60/40) semi-IPNs it appears that pure PCHMA and pure PIB phase are of minor proportion (near to 5%) very different from the introduced amounts. This means indeed that intimately combined phases (PIB/PCHMA (50/50) if all the grey shades are combined, although finer analysis might be tricky) between the two partners compose the majority of the samples.

Phase co-continuity has been also observed on the corresponding full PIB/PCHMA IPNs by AFM analyses in tapping mode reported earlier [26]. From these images, the PIB and PCHMA rich phase domain size in the IPN has been estimated at about 0.1 µm which is of the same order of magnitude than in semi-IPNs containing less than 50 wt% PCHMA.

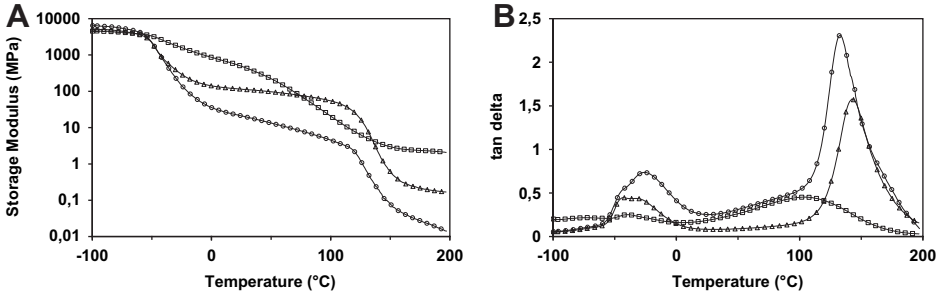

Fig. 9. Storage modulus (A) and tanδ (B)-temperature curves recorded on PIB/PCHMA (50/50) (△) semi-IPN, (□) IPN and (○) blend.

3.10. PIB/PCHMA semi-IPN, blend and full IPN comparison

Finally, a comparison can be drawn between the thermomechanical properties of a semi-IPN, a blend and a full PIB/PCHMA IPN with identical 50/50 weight proportions (Fig. 9).

All samples show an identical glassy phase below −50 °C, which is the onset of the PIB rich phase mechanical relaxation. With increasing temperature, the moduli decrease with different trends between −70 and 110 °C according to the nature of the sample (Fig. 9A). Indeed, the IPN modulus decreases regularly from 3000 to 2 MPa whereas the blend and the semi-IPN moduli decrease more sharply down to a pseudo plateau. The modulus at the pseudo plateau for the semi-IPN (135 MPa) is ten times higher than that of the blend (13 MPa). At about 110 °C, the storage moduli decrease again which correspond to the beginning of the PCHMA phase mechanical relaxation in the three samples. The moduli of the semi-IPN and IPN reach a third plateau extending to 200 °C whereas the blend curve is characterized by a drop at 150 °C indicating flowing of the material. Above 150 °C the rubber plateau of the IPN is ten times higher that of the semi-IPN. This difference clearly arises from the PIB-PCHMA interpenetration highlighted with the tanδ-temperature curve of the IPN (Fig. 9B). A broad (0 °C–170 °C) relaxation with a low intensity ($\tan\delta = 0.7$) is detected with a maximum at 100 °C, a temperature located between those of the mechanical relaxations of PIB and PCHMA. This relaxation is characteristic of an interpenetrated PIB and PCHMA network phase [26]. Although both IPN and semi-IPN exhibit phase co-continuity, their thermomechanical behaviour is quite different. The interaction between the phases is more important in the IPN than in the semi-IPN although the PIB remains entrapped in both cases. In addition, both architectures lead to a material without flow by contrast with the corresponding blend.

4. Conclusion

In this study, it was shown that it is possible to entrap polyisobutene as efficiently in a semi-IPN architecture as in cross-linkable telechelic PIB based full IPN architecture as far as the cold flow occurrence is suppressed. Indeed, PIB based semi-IPNs showing no flow and higher mechanical properties than those of linear PIB have been elaborated by entrapping this linear polymer inside a PCHMA network. The morphology of these new materials compares with that of corresponding IPNs, in the sense that phase co-continuity is obtained on a large composition range. Moreover, the PIB gas permeation properties are unexpectedly improved in the PCHMA semi-IPN architecture.

Two of the main advantages of these new semi-IPN architectures are, on the one hand, they do not require telechelic PIB oligomers as synthetic precursors. On the other hand, no solvent is required in the described synthesis because middle molecular weight linear PIB can be dissolved in CHMA monomer. Furthermore, it was shown that the synthesis conditions, in particular the temperature as a direct control of the reacting mixture viscosity, is an important parameter that allows modifying the phase separation degree in the final material.

It would be interesting to generalize the possibility of immobilizing PIB in any given material studying other partner networks the properties of which will be associated to those of PIB. Thus, a large range of PIB based new materials showing tuneable mechanical properties and tuneable tack, for instance, could be elaborated. These other materials will be subjected in a forthcoming paper.

Acknowledgements

The authors thank BASF for financial support, and particularly Dr. P. Hanefeld, Dr. K. Mühlbach, Dr. N. Hildebrandt and Dr. H. König who very actively supported this research, provided the polyisobutene samples and carried out TEM and permeation experiments.

References

[1] Othmer K. In Encyclopedia of Chemical Technology. New York: J. Wiley and Sons; 1998.
[2] Park D, Keszler B, Galiatsatos V, Kennedy JP. J Appl Polym Sci 1997;66:901–10.
[3] Kramer O, Greco R, Neira RA, Ferry JD. J Polym Sci 1974;12:2361–74.
[4] Kunal K, Paluch M, Roland CM, Puskas JE, Chen Y, Sokolov AP. J Polym Sci Part B Polym Phys 2008;46:1390–9.
[5] Groenewolt M, Brezinski T, Schlaad H, Antonietti M, Groh PW, Iván B. Adv Mater 2005;17:1158–62.
[6] Puskas JE, Antony P, El Fray M, Altstädt V. Eur Polym J 2003;39:2041–9.
[7] Kennedy JP, Midha S, Teunogaes Y. Macromolecules 1993;26(3):429–35.
[8] Jacob S, Kennedy JP. Polym Bull 1998;41:167–74.
[9] Kennedy JP, Kurian J. J Polym Sci Part A Polym Chem 1990;28:3725–38.
[10] Puskas JE, Chen Y, Dahman Y, Padavan D. J Polym Sci Part A Polym Chem 2004;42:3091–109.
[11] Storey RF, Chisholm BJ, Masse MA. Polymer 1996;37(14):2925–38.
[12] Storey RF, Baugh DW. Polymer 2001;42(6):2321–30.
[13] Storey RF, Baugh DW. Polymer 2000;41(9):3205–11.
[14] Kwee T, Taylor SJ, Mauritz KA, Storey RF. Polymer 2005;46(12):4480–91.
[15] Sherman MA, Kennedy JP, Ely DL, Smith D. J Biomater Sci Polym 1999;10(3):259–69.
[16] Sherman MA, Kennedy JP. J Polym Sci Part A Polym Chem 1998;36:1901–10.
[17] Sherman MA, Kennedy JP. J Polym Sci Part A Polym Chem 1998;36:1891–9.
[18] Ivan B, Almdal K, Mortensen K, Johannsen I, Kops J. Macromolecules 2001;34(6):1579–85.
[19] Scherble J, Thomann R, Iván B, Mülhaupt R. J Polym Sci Part B Polym Phys 2001;39:1429–36.
[20] Chen D, Kennedy JP, Allen AJ. J Macromol Sci Chem 1988;25(4):389–401.
[21] Erdodi G, Ivan B. Chem Mater 2004;16(6):959–62.
[22] Sperling LH, Mishra V. IPNs Around the World: Science and Engineering. New York: J. Wiley and Sons; 1997. pp. 1–25.
[23] Sperling L.H., In: Interpenetrating Polymer Networks. Sperling L.H., Klempner D., Utracki L.A., editors. Washington DC: Adv Chem Ser 239, ACS, 1994. pp. 3–38.
[24] Vancaeyzeele C, Fichet O, Boileau S, Teyssié D. Polymer 2005;46(18):6888–96.
[25] Vancaeyzeele C, Fichet J, Laskar O, Boileau S, Teyssié D. Polymer 2006;47(6):2046–60.
[26] Vancaeyzeele C, Fichet O, Amana B, Boileau S, Teyssié D. Polymer 2006;47(17):6048–56.
[27] Teyssié D, Vancaeyzeele C, Laskar J, Fichet O, Boileau S, Blackborow JR, Rath HP, Lange A, Lange G, Mach H, Hiller M. WO2005019285.
[28] Hanefeld P, Hildebrandt N, Muehlbach K, Mach H, Walter HM, Teyssié D, Vancaeyzeele C, Fichet O, Davion B. WO2008155395.
[29] Ruzette AVG, Mayes AM. Macromolecules 2001;34:1894–907.
[30] Stansbury JW, Dickens SH. Dental Mater 2001;17:71–9.
[31] Denisov ET, Denisova TG, Pokidova TS. Handbook of Free Radical Initiators. John Wiley & Sons, Inc; 2003. pp 139 and 154.
[32] Moad G, Solomon DH. The chemistry of radical polymerization. Elsevier; 2006.
[33] Plazek DJ, Chay IC, Ngai KL, Roland CM. Macromolecules 1995;28(19):6432–6.
[34] Ngai KL, Plazek DJ. Macromolecules 2002;35(24):9136–41.
[35] Frick B, Richter D. Phys Rev B 1993;47(22):14795–804.
[36] Darras V, Peralta S, Boileau S, Teyssié D, Fichet O. Polym Int 2010;59(6):743–8.
[37] Rubinstein M, Colby RH. Polymer Physics. New York: Oxford University Press Inc; 2003 [chapter 9].
[38] Lohse DJ. J Macromol Sci C 2005;45:289–308.
[39] Sperling LH. Introduction to physical polymer science. 4th ed. Wiley; 2006. pp. 394–395.
[40] Seferis JC. In: Brandrup J, Immergut EH, Grulke EA, editors. Polymer Handbook. 4th ed. Wiley-Interscience Publication; 1999 [chapter 4].
[41] O'Connora AE, Willenbacher N. Int J Adhes Adhes 2004;24:335–46.
[42] Chang MCO, Thomas DA, Sperling LH. J Appl Polym Sci 1987;34:409–22.
[43] Flory PJ, Rehner JJ. Chem Phys 1943;11:521–6.
[44] Widmaier JM, Sperling LH. J Appl Polym Sci 1982;27:3513–25.
[45] Hourston DJ, Schäfer FU. Polymer 1996;37(16):3521–30.
[46] Kim SC, Klempner D, Frisch KC, Frisch LH. Macromolecules 1977;10(6):1187–91.
[47] Akay M, Rollins SN. Polymer 1993;34(9):1865–73.
[48] Kerner EH. Proc Phys Soc London B 1956;69:808–13.
[49] Budiansky B. J Mech Phys Solids 1965;13:223–32.
[50] Coran AY, Patel R. J Appl Polym Sci 1976;20:3005–16.
[51] Yeo JK, Sperling LH, Thomas DA. Polym Eng Sci 1981;21(1):696–702.
[52] Davies WEA. J Phys D Appl Phys 1971;4:1176–81.
[53] Fontanille M, Gnanou Y. Chimie et physico-chimie des polymères. In: Dunod, editor; 2002 [chapter 5].
[54] Qin CL, Cai WM, Cai J, Tang DY, Zhang JS, Qin M. Mater Chem Phys 2004;85(2/3):402–9.
[55] Donatelli AA, Sperling LH, Thomas DA. Macromolecules 1976;9:671–5.
[56] Fay JJ, Thomas DA, Sperling LH. J Appl Polym Sci 1991;43:1617–23.